Research Square

Preprints are preliminary reports that have not undergone peer review.
They should not be considered conclusive, used to inform clinical practice,
or referenced by the media as validated information.

Constructed a stable coordination polymer for highly efficient and selective capture of thorium

qinghua hu

huqinghua@jgsu.edu.cn

Jinggangshan University

Yeliang gao

Jinggangshan University

jin guo

Jinggangshan University

limin liu

Jinggangshan University

Research Article

Keywords: Coordination polymer, Adsorption, Hydrophobic groups, Thorium(IV), Radioactive wastewater treatment

Posted Date: October 23rd, 2026

DOI: https://doi.org/10.21203/rs.3.rs-11188074/v1

License: This work is licensed under a Creative Commons Attribution 4.0 International License.
Read Full License

Additional Declarations: No competing interests reported.

Abstract

The efficient separation of thorium (Th) from chemically similar rare earth elements (REEs) is technically challenging. In this work, a stable coordination polymer (Ni-tfc-CP) was fabricated by adopting the strategy of in-situ incorporation of hydrophobic groups. Ni-tfc-CP exhibits excellent structural stability over a wide pH range of 2–11 and under high-temperature conditions up to 247°C. The abundant carboxyl oxygen active binding sites on the surface of Ni-tfc-CP, provides favorable environment for Th(IV) uptake. The maximum adsorption capacity was calculated to 518.9 mg g^{-1}, by fitting the equilibrium data to the Langmuir model. Moreover, it showed an ultra-fast adsorption rate and reached equilibrium within 5 minutes. Notably, competitive tests confirmed the superior selectivity of Ni-tfc-CP for Th(IV), with a high distribution coefficient of 6×10^5 mL g^{-1}. This study provides meaningful guidance for the rational development of functional materials toward nuclide separation.

Introduction

Against the backdrop of booming rare-earth industry, large quantities of tailings containing radioactive thorium (Th) are produced during ore beneficiation and separation processes [1–4]. Thorium embedded in rare-earth tailings may enter the ecological environment via leaching, dust diffusion and surface runoff, bringing potential threats to the ecological system and human health [5–7]. Therefore, effective removal of radioactive thorium from rare-earth tailings is of great practical significance for environmental safety. Nevertheless, thorium removal still faces multiple technical and practical challenges owing to the complex mineral composition of tailings.

Adsorption has become a research hotspot in the field of radioactive nuclide separation due to its simple operation, high removal efficiency and easy integration with existing processes [8, 9]. The core of adsorption technology lies in the design of adsorbent materials. Although traditional adsorbents such as activated carbon[10–12], zeolite composite [13], metal oxide [14–16], and ion exchange resins [17, 18] have been widely used, they often face challenges such as limited adsorption capacity, low selectivity, difficult regeneration or insufficient stability when dealing with actual radioactive waste liquid with complex components [19–21]. To address these issues, researchers have focused on the development of advanced porous materials with well-defined pore structures and designable surfaces, such as metal-organic frameworks (MOFs), Covalent Organic Frameworks (COFs), have shown excellent potential in the separation of actinide nuclides [22–24]. But their often limited in practical applications by harsh synthesis conditions, difficulty in large-scale preparation, high cost, and insufficient framework stability in extreme environments such as strong acid and high irradiation [25, 26]. Thus, developing materials that maintain high stability, large adsorption capacity, and outstanding selectivity under real water matrix conditions is urgently needed.

Coordination polymers, assembled from multifunctional organic linkers and metal ions or metal clusters, exhibit potential applications in radionuclide remediation, due to their abundant adsorption sites, highly designable/modifiable structures, and good batch reproducibility [27–30]. Shi et al. employed carboxyl-

grafted UiO-66 for the removal of thorium from solution [31]. The results show that although the specific surface area and pore volume decrease significantly, the adsorption performance toward Th(IV) is greatly enhanced. UiO-66-$(COOH)_2$ delivers an adsorption capacity of 350 mg g^{-1} for Th(IV), which is considerably higher than those of UiO-66 and UiO-66-COOH. Mechanistic studies reveal strong coordination interactions between carboxyl groups and Th(IV). Subsequently, Xiao et al. reported an oxygen-rich ion trap (IEF-11), further confirming the unique chelating interaction between oxygen and Th(IV) [32]. However, these metal-organic framework materials suffer from drawbacks such as low adsorption capacity and poor chemical stability, which makes them difficult for practical engineering applications.

To address this challenge, researchers try to introduce hydrophobic groups into the structure to enhance the stability of materials [33]. For example, Ding et. al. systematically summarized various strategies for enhancing MOF stability, pointing out that introducing hydrophobic groups into ligands can construct hydrophobic microenvironments within pores and block the attack of water molecules on metal nodes [26]. Abbas et al. demonstrated that the incorporation of fluorine-containing groups into rare earth metal–organic frameworks (RE-MOFs) enhances the water stability of the materials [34]. Therefore, 4-trifluoromethylnicotinic acid, which bearing carboxylic acid and trifluoromethyl substituents, was chosen as the organic ligand to provide active sites and boost material stability via hydrophobic interactions.

Herein, a chemically stable coordination polymer (Ni-tfc-CP) was synthesized from $Ni(OAc)_2{\cdot}4H_2O$ and 4-trifluoromethylnicotinic acid (Fig. 1). The Ni-tfc-CP exhibits fast adsorption rate, high removal efficiency, excellent selectivity and superior cyclic stability toward Th(IV). It provides a facile and low-cost strategy for developing stable adsorbents, with good application potential in thorium-containing radioactive wastewater treatment.

Experimental

Chemical reagents and materials

Nickel(II) acetate tetrahydrate ($Ni(OAc)_2{\cdot}4H_2O$, 98%) was obtained from Anhui Senmei Technology Co., Ltd., and 4-trifluoromethylnicotinic acid (Htfc, 98%) was purchased from Shanghai Titan Scientific Co., Ltd. Methanol and deionized water were adopted as solvents throughout the experiments.

Synthesis of Ni-tfc-CP

The Ni-tfc coordination polymer (Ni-tfc-CP) was prepared by a hydrothermal method. Briefly, $Ni(OAc)_2{\cdot}4H_2O$ (0.1 mmol,24.9 mg), Htfc (0.1 mmol,19.1 mg), 3 mL water, and 1 mL methanol were added to a PTFE reactor. Then heated at 140°C for 72 h, and cooled to room temperature within 24 h, and green block crystals were obtained.

Adsorption Experiments

Batch adsorption experiments were carried out with the solid/liquid ratio of 1 g L^{-1}. The influences of solution pH, adsorption kinetics, isotherms, selectivity and reusability were systematically studied. All detailed experimental procedures, test conditions and calculation formulas are presented in the Supporting Information.

Results and Discussion

Structural Characterization and Stability Analysis

The structure Ni-tfc-CP was characterized via scanning electron microscopy, powder X-ray diffraction, and Fourier-transform infrared spectroscopy. SEM (Fig. S1) images show a block morphology with a diameter of ~ 100 μm. As shown in Fig. 2a, Ni-tfc-CP exhibited distinct diffraction peaks at 7.5° and 24.2–27.9°, significantly differ from those of the free Htfc ligand, confirming the formation of a new phase rather than a simple precursor mixture. In the FT-IR spectrum (Fig. 2b), the stretching vibration of C = N are located at ~ 1139 cm^{-1} [35]. After coordination, the C = N in Ni-tfc-CP has great blue shift to 1146 cm^{-1}. A new characteristic band at 467 cm^{-1} is assigned to Ni-N stretching [36], confirms the pyridine nitrogen in Htfc coordinates with Ni^{2+} ions. The asymmetric stretching of COOH at 1700 cm^{-1} was obviously weakened, as well as shifted to 1693 cm^{-1} [37], indicate the carboxyl functional groups of Htfc coordination with Ni ions. In the N 1s spectra of Ni-tfc-CP, the peaks at 399.9 eV and 399.4 corresponding to Ni-N bond and C = N signal (Fig. 2c) [38]. As shown in Fig. 2d, two peaks can be observed at 530.8 eV and 531.6 eV in O 1s XPS spectra were attributed to Ni-O and COOH, respectively [39]. Moreover, XPS data show that the atomic ratios of N and O to Ni are 3 and 7, respectively. (Table S1). Therefore, it can be concluded that each Ni^{2+} ion is coordinated by one pyridine N atom from one Htfc ligand, four carboxylate O atoms from two Htfc ligands, and one water molecule, adopting a six-coordinate configuration.

To evaluate the structural stability of Ni-tfc-CP under different environmental conditions, the pH stability was investigated by immersing the sample in aqueous solutions with different pH values. The PXRD patterns (Fig. S2) show that the main characteristic diffraction peaks of Ni-tfc-CP remain almost unchanged across the entire pH range of 2–11, suggesting that the framework of Ni-tfc-CP is well preserved under these conditions. The FT-IR spectra (Fig. S3) further confirm this conclusion, as the characteristic absorption bands of the functional groups in Ni-tfc-CP do not show obvious shifts or disappearances after treatment at different pH values. This superior chemical stability of Ni-tfc-CP is primarily ascribed to the strongly hydrophobic trifluoromethyl groups introduced at ortho positions.

The thermal stability of Ni-tfc-CP was studied by thermogravimetric analysis (TGA) under a nitrogen atmosphere. The TGA curve reveals that Ni-tfc-CP maintains its structural integrity up to approximately 247°C, with only a slight weight loss of 1.96% below this temperature, which is attributed to the removal of adsorbed water or residual solvent molecules (Fig. S4). It indicates that Ni-tfc-CP possesses good

thermal stability, sufficient to withstand the temperature conditions encountered in typical adsorption applications.

Adsorption Performance

The solution pH is a critical factor affecting the adsorption behavior, as it influences both the surface charge of the adsorbent and the existing species of Th(IV) [40]. Accordingly, we investigated the Th(IV) removal efficiency of Ni-tfc-CP across aqueous solutions of varying pH. As shown in Fig. 2a, the removal efficiency of Ni-tfc-CP for Th(IV) increases gradually with increasing pH from 2.5 to 4.0, reaching a maximum value (99.8%) at pH 4.0, and then slightly decreases at pH 4.5. This trend can be attributed to the competition between H^+ and Th(IV) ions for active sites at low pH, as well as the hydrolysis of Th(IV) ions at higher pH [41]. Therefore, pH 4.0 was selected as the optimal condition for subsequent adsorption experiments.

To investigate the ability of Ni-tfc-CP to capture Th(IV), isothermal adsorption experiments were conducted. As shown in Fig. 2b, the Langmuir isotherm adsorption model fits the experimental data better, with a higher fitting coefficient (R^2 = 0.99, Table S2), suggesting uniform adsorption on a monolayer surface. The maximum adsorption capacity of Ni-tfc-CP was calculated to be 518.9 mg g^{-1}, which is close to the experimental value (497.7 mg g^{-1}), demonstrating the high adsorption potential of Ni-tfc-CP for Th(IV) [42]. Energy dispersive X-ray spectroscopy (EDS) mapping confirms that Th(IV) ions penetrate the material structure and distribute uniformly across the samples (Fig. S5).

The rapid kinetics of adsorbents are essential for the effective sequestration of radionuclides. Therefore, kinetic experiments for the Th(IV) capture by Ni-tfc-CP were implemented. As presented in Fig. 2c, the thorium removal efficiency increases rapidly within the first few minutes and reaches equilibrium within 5 minutes, surpasses most adsorbents (Table S3), such as, Ca-NDA (50 min) [43], IEF-11 (100 min) [32], and DBT-DHTA-Cd (30 min) [44] The kinetic data can be better fitted with the pseudo-second order kinetic model with the R^2 of 0.99 (Fig. S6-7, Table S4), which suggests that chemical adsorption plays a dominant role in the adsorption of Th (IV) by Ni-tfc-CP [45]. The rapid equilibration indicates that Ni-tfc-CP is well suited to long-term treatment of radioactive wastewater.

To evaluate the practical applicability of Ni-tfc-CP, adsorption selectivity experiments were carried out in the presence of various competing metal ions (Na(I), Mg(II), Al(III), K(I), Ca(II), Cr(III), Mn(II), Fe(III), Co(II), Cu(II), Zn(II), Pd(II), Cd(II), Hg(II), Pb(II), La(III), Ce(III), Pr(III), Nd(III), Sm(III), Eu(III), Tb(III), Dy(III), Ho(III), Er(III), Lu(III)). As depicted in Fig. 2d, Th(IV) delivers an extraordinarily large distribution coefficient (K_d) of 6.0×10^5 mL/g, which is over three orders of magnitude greater than other metal species. Such a huge discrepancy in (K_d) unambiguously demonstrates that Ni-tfc-CP achieves exceptional adsorption selectivity toward Th(IV) against a broad spectrum of interfering metal ions [46].

We also investigated the recycling performance of Ni-tfc-CP for Th(IV) removal. The desorption experiments were then carried out with a 0.1 mol/L Na_2CO_3 solution. As illustrate in Fig. S8, the removal

efficiency of Th(IV) remains nearly 100% even after five cycles, demonstrating that Ni-tfc-CP has excellent stability and recyclability.

Elucidation of the Th(IV) Adsorption Mechanism

The XRD, FT-IR, and XPS were applied to evaluate the structure-performance relationship of Ni-tfc-CP in the effective capture of thorium ions. The obtained PXRD patterns of Ni-tfc-CP@Th exhibited consistent diffraction peaks with the pristine ones (Fig. S9), indicating that the adsorption of Th(IV) would not disrupt the structures. After adsorption Th(IV), the signal of -COOH shows a large blue shift of 16 cm^{-1} (from 1716 cm^{-1} to 1700 cm^{-1}). A weak band at ~ 505 cm^{-1} corresponds to Th–O stretching vibration (Fig. 4a). These results illustrating that the robust interaction between thorium and carboxyl groups in Ni-tfc-CP. To further examine the binding behavior of thorium ions in Ni-tfc-CP, XPS measurement was carried out. The full survey spectrum shows a distinct Th 4f signal after adsorption, verifying the introduction of Th(IV) (Fig. 4b). The high-resolution Th 4f spectrum displays two characteristic peaks at 334.1 eV and 343.4 eV, corresponding to Th $4f_{7/2}$ and Th $4f_{5/2}$ [47], respectively (Fig. 4c), indicating that thorium species kept tetravalent oxidation states loaded without redox reaction. In the high-resolution O 1s spectra (Fig. 4d), the signal of COOH at 531.6 eV had a significant positive shift to 532.5 eV [48], after capturing thorium. Meanwhile, a new peak at 529.9 eV is assigned to the Th–O bond [12, 31], proving strong interactions between thorium and the carboxyl in Ni-tfc-CP.

Conclusion

In summary, A new stability coordination polymer Ni-tfc-CP with abundant carboxyl functional groups was constructed for Th(IV) capture. The introduction of hydrophobic trifluoromethyl groups can greatly enhance the chemical resistance of compound Ni-tfc-CP. Owing to the abundant carboxyl groups in its structure, Ni-tfc-CP demonstrated impressive adsorption capacities of 553 mg g^{-1}. Remarkably, Ni-tfc-CP exhibits superior selectivity for Th(IV), achieving a distribution coefficient of 6×10^5 mL g^{-1}, 4–5 orders of magnitude higher than competing ions. This work highlights the in-situ introduction of hydrophobic moieties into the framework to enhance stability and adsorption performance, offering a promising strategy for the remediation of Th(IV)-contaminated water.

Declarations

Acknowledgements We acknowledge financial support from the National Natural Science Foundation of China (22406072), Natural Science Foundation of Jiangxi Province (20242BAB20101 and 20252BAC240311), Natural Science Foundation of Jinggangshan University (JZ2502 and JZB2315).

Author Contributions Qing-Hua Hu: Writing – original draft, Visualization, Methodology, Investigation, Data curation, Conceptualization. Ye-Liang Gao: Validation, Investigation, Formal analysis, Data curation.

Jin Guo: Validation, Investigation, Data curation. Li-Min Liu: Writing – review & editing, Supervision, Funding acquisition, Conceptualization.

Competing interests The authors declare no competing interests.

Data Availability The datasets generated and analyzed during the current study are available from the corresponding author on reasonable request.

References

1. H. Zhou, Y. Wang, Q. Yu, R. Li, Q. Huang, D. Huang, S. Ding, EDTA-derived tetraamide ligands for highly selective separation of thorium over uranium and rare earths. Inorg. Chem. 65, 4939–4951 (2026).
2. M.A. Khan, S. Huang, X. Du, Y. Yang, Y. Li, Y. Yuan, N. Wang, Bio-metal-organic framework with Nano-window traps for ultra-selective thorium separation. Sep. Purif .Technol. 392, 137179 (2026).
3. L. Peng, Q. Peng, T. Jin, Z. Liu, Y. Qian, Highly efficient capture of thorium ion by citric acid-modified chitosan gels from aqueous solution. Chinese Chem. Lett. 108891 (2023).
4. M.F. Hamza, V. Wei, M.S. Khalafalla, N.S. Abed, A. Fouda, K.Z. Elwakeel, E. Guibal, N.A. Hamad, U(VI) and Th(IV) recovery using silica beads functionalized with urea- or thiourea-based polymers – Application to ore leachate. Sci. Total Environ. 821, 153184 (2022).
5. Y. Cui, H. Lu, H. Hou, Y. Bai, J.Yang, Y. Li, J. Qiu, S. Wang, J. Lin, Dissolution-Recrystallization: A novel mechanism for fluorochromic detection of Th^{4+} using color-tunable luminescent metal-organic frameworks. Angew. Chem. Int. Ed. 63, e202410453 (2024).
6. C. Lin, H. Wang, Y. Wang, Z. Cheng, Selective solid-phase extraction of trace thorium(IV) using surface-grafted Th(IV)-imprinted polymers with pyrazole derivative. Talanta 81, 30–36 (2010).
7. D. Emre, Zorer Ö. Selçuk, A. Bilici, Polyserotonin-functionalized graphitic carbon nitride nanosheets as composite adsorbents for uranium (VI) and thorium (IV) removal. J. Polym. Environ. 34, 113 (2026).
8. S. Ni, Y.T. Li, X. Xu, S. Hou, X. Lü, Q.Y. Yang A fluorinated zinc-based metal-organic framework for efficient separation of butane isomers via pore engineering. Small Methods 9, 2500027 (2025).
9. J. Cui, Z. Qiu, Z. Yang, A. Jin, X. Cui, L. Yang, H. Xing, One-step butadiene purification in a sulfonate-functionalized metal–organic framework through synergistic separation mechanism. Angew. Chem. Int. Ed. 63, e202403345 (2024).
10. Z. Wang, A.T. Brown, K. Tan, Y.J. Chabal, K.J. Balkus, Selective extraction of thorium from rare earth elements using wrinkled mesoporous carbon. J. Am. Chem. Soc. 140, 14735–14739 (2018).
11. Z.W. Huang, Z.J. Li, L.R. Zheng, W.S. Wu, Z.F. Chai, W.Q. Shi, Adsorption of Eu(III) and Th(IV) on three-dimensional graphene-based macrostructure studied by spectroscopic investigation. Environ. Pollut. 248, 82–89 (2019).

12. Y. Gao, L. Xu, M. Zhang, Q. Zhang, Z. Yang, J. Yang, Z. Xu, Y. Lv, Y. Wang, Ultra-selective ion sieve for thorium recovery from rare earth elements using oxygen-rich microporous carbon adsorption. J. Hazard. Mater. 417, 126115 (2021).
13. A.K. Kaygun, S. Akyil, Study of the behaviour of thorium adsorption on PAN/zeolite composite adsorbent. J. Hazard. Mater. 147, 357–362 (2007).
14. S. Abbasizadeh, A.R. Keshtkar, M.A. Mousavian, Preparation of a novel electrospun polyvinyl alcohol/titanium oxide nanofiber adsorbent modified with mercapto groups for uranium(VI) and thorium(IV) removal from aqueous solution. Chem. Eng. J. 220, 161–171 (2013).
15. L.Y. Yuan, Z.Q. Bai, R. Zhao, Y.L. Liu, Z.J. Li, S.Q. Chu, L.R. Zheng, J. Zhang, Y.L. Zhao, Z.F. Chai, W.Q. Shi, Introduction of bifunctional groups into mesoporous silica for enhancing uptake of thorium(IV) from aqueous solution. ACS Appl. Mater. Interfaces 6, 4786–4796 (2014).
16. Ü.H. Kaynar, M. Ayvacıklı, Ü. Hiçsönmez, Kaynar S. Çam, Removal of thorium (IV) ions from aqueous solution by a novel nanoporous ZnO: Isotherms, kinetic and thermodynamic studies. J. Environ. Radioactiv. 150, 145–151 (2015).
17. Y. Lu, Y. Bi, Y. Bai, W. Liao, Extraction and separation of thorium and rare earths from nitrate medium with p-phosphorylated calixarene. J. Chem. Technol. Biotechnol. 88, 1836–1840 (2013).
18. J. Su, X. Guo, Y. Gao, S. Wu, R. Xu, X. Sun, Recovery of thorium and rare earths from leachate of ion-absorbed rare earth radioactive residues with N1923 and Cyanex® 572. J. Rare Earth 39, 1273–1281 (2021).
19. Q. Sun, L. Zhu, B. Aguila, P.K. Thallapally, C. Xu, J. Chen, S. Wang, D. Rogers, S. Ma, Optimizing radionuclide sequestration in anion nanotraps with record pertechnetate sorption. Nat. Commun. 10, 1646 (2019).
20. Y. Song, J. Phipps, C. Zhu, S. Ma, Porous materials for water purification. Angew. Chem. Int. Ed. 62, e202216724 (2023).
21. Z. Huang, H. Dong, N. Yang, H. Li, N. He, X. Lu, J. Wen, X. Wang Bifunctional phosphorylcholine-modified adsorbent with enhanced selectivity and antibacterial property for recovering uranium from seawater. ACS Appl. Mater. Interfaces 12, 16959–16968 (2020).
22. Y. Wang, X. Ye, Q. Zhang, W. Han, X. Liu, H. Zhang, H. Liu, Z. Wu, G. Shi Unveiling the adsorption behavior and mass transfer mechanism of Rb^+ and Cs^+ adsorption on FeMn-MOF. Chem. Eng. J. 502, 157999 (2024).
23. A.M. Song, M.J. Yang, Z. Wu, Q. Yang, B. Lin, R.P. Liang, J.D. Qiu, Rational designed metal–organic framework with nanocavity traps for selectively recognizing and separating of radioactive thorium in rare earth wastewater. Adv. Funct. Mater. 34, 2406932 (2024).
24. S. Chen, K. Yu, X. Su, H. Hu, J. Zhao, B. Wang, Z. Wen, A. Saleem, M. Wang, S. Xiao, Y. Gao, Engineering dual-active N and O Sites in covalent organic frameworks for ultrahigh and selective thorium removal. Adv. Funct. Mater. 36, e75216 (2026).
25. A.A. Alqadami, M. Naushad, Z.A. Alothman, A.A. Ghfar, Novel metal–organic framework (MOF) based composite material for the sequestration of U(VI) and Th(IV) metal ions from aqueous

environment. ACS Appl. Mater. Interfaces 9, 36026–36037 (2017).

26. M. Ding, X. Cai, H.L. Jiang, Improving MOF stability: approaches and applications. Chem. Sci. 10, 10209–10230 (2019).
27. P.M. Bhatt, V. Guillerm, S.J. Datta, A. Shkurenko, M. Eddaoudi, Topology meets reticular chemistry for chemical separations: MOFs as a case study. Chem 6, 1613–1633 (2020).
28. M. Dincă, J.R. Long, Introduction: porous framework chemistry. Chem. Rev. 120, 8037–8038 (2020).
29. W. Fan, X. Zhang, Z. Kang, X. Liu, D. Sun, Isoreticular chemistry within metal–organic frameworks for gas storage and separation. Coordin. Chem. Rev. 443, 213968 (2021).
30. X. Zhang, J. Maddock, T.M. Nenoff, M.A. Denecke, S. Yang, M. Schröder Adsorption of iodine in metal–organic framework materials. Chem. Soc. Rev. 51, 3243–3262 (2022).
31. N. Zhang, L.Y. Yuan, W.L. Guo, S.Z. Luo, Z.F. Chai, W.Q. Shi, Extending the use of highly porous and functionalized MOFs to Th(IV) capture. ACS Appl. Mater. Interfaces 9, 25216–25224 (2017).
32. X. Chen, G. Li, S. Xiao, W. Xue, X. Zhao, Q. Yang, Efficient capture of Th(IV) and U(VI) by radiation-resistant oxygen-rich ion traps based on a metal–organic framework. ACS Appl. Mater. Interfaces 15, 25029–25040 (2023).
33. D. Sheng, L. Zhu, X. Dai, C. Xu, P. Li, C.I. Pearce, C. Xiao, J. Chen, R. Zhou, T. Duan, O.K. Farha, Z. Chai, S. Wang, Successful decontamination of $^{99}TcO_4^-$ in groundwater at legacy nuclear sites by a cationic metal-organic framework with hydrophobic pockets. Angew. Chem. Int. Ed. 58, 4968–4972(2019).
34. M. Abbas, B. Murari, S. Sheybani, M. Joy, K.J. Balkus, Synthesis and characterization of highly fluorinated hydrophobic rare–earth metal–organic frameworks (MOFs), Mater. 17, 4213 (2024).
35. M. Shi, D. Chen, X. Zhao, Z. Ren, G. Yu, C. Wang, R. Zhao, G. Zhu, Robust and porous cationic polymeric network nanofiber membrane with high alkaline stability for efficient $^{99}TcO_4^-/ReO_4^-$ removal. Chem. Eng. J. 506, 160140 (2025).
36. G. Cai, P. Cui, W. Shi, S. Morris, S.N. Lou, J. Chen, J.H. Ciou, V.K. Paidi, K.S. Lee, S. Li, P.S. Lee, One-dimensional π-d conjugated coordination polymer for electrochromic energy storage device with exceptionally high performance. Adv. Sci. 7, 1903109 (2020).
37. J. Wu, Z. Li, H. Tan, S. Du, T. Liu, Y. Yuan, X. Liu, H. Qiu, Highly selective separation of rare earth elements by Zn-BTC metal–organic framework/nanoporous graphene via in situ green synthesis. Anal. Chem. 93, 1732–1739 (2021).
38. J.H. Cho, J. Ma, C. Lee, J.W. Lim, Y. Kim, H.Y. Jang, J. Kim, M.G. Seo, Y. Choi, Y.J. Jang, S.H. Ahn, H.W. Jang, S. Back, J.L. Lee, S.Y. Kim, Crystallographically vacancy-induced MOF nanosheet as rational single-atom support for accelerating CO_2 electroreduction to CO. Carbon Energy 6, e510 (2024.
39. C. Shuai, C. Kong, Y. Li, L. Zhang, C. Qi, Z. Mo, 3D flower-like bimetallic Ni–Co metal–organic framework as an electrocatalyst for the oxygen evolution reaction. RSC Adv. 14, 18367–18372 (2024).

40. Y. Huang, H. Zheng, H. Li, Z. Zhang, C. Zhao, Q. Gou, Y. Liu, Highly effective and selective adsorption of thorium(Ⅳ) from aqueous solution using mesoporous graphite carbon nitride prepared by sol–gel template method. Chem. Eng. J. 410, 128321 (2021).
41. X. Liu, F. Gao, T. Jin, K. Ma, H. Shi, M. Wang, Y. Gao, W. Xue, J. Zhao, S. Xiao, Y. Ouyang, G. Ye, Efficient and selective capture of thorium ions by a covalent organic framework. Nat. Commun. 14, 5097 (2023).
42. S.P., N P, Perumal I, G S, B M, M P, Adsorption of thorium (IV) from aqueous solutions using mesoporous TiO_2: Kinetics, isotherm and thermodynamics. Chem. Phys. Impact 8, 100638 (2024).
43. M.J. Yang, A.M. Song, Q. Yang, Z. Wu, B. Lin, R.P. Liang, J.D. Qiu, One-step open-ring strategy for constructing sandwich-like metal–organic framework with highly selective removal of thorium. Chem. Eng. J. 505, 159718 (2025).
44. A.M. Song, M.J. Yang, Z. Wu, Q. Yang, B. Lin, R.P. Liang, J.D. Qiu, Rational designed metal–organic framework with nanocavity traps for selectively recognizing and separating of radioactive thorium in rare earth wastewater. Adv. Funct. Mater. 34, 2406932 (2024).
45. B. Zheng, X. Lin, X. Zhang, D. Wu, K. Matyjaszewski, Emerging functional porous polymeric and carbonaceous materials for environmental treatment and energy storage. Adv. Funct. Mater. 30, 1907006 (2020).
46. S. Sheybani, M. Abbas, M. Joy, C.R. Brewer, A.V. Walker, K.J. Balkus, Selective extraction of thorium using nanoporous sulfate-functionalized fluoro-bridged holmium metal–organic frameworks. ACS Appl. Nano .Mater. 8, 18762–18771 (2025).
47. B. Chen, L. Ding, Y. Wang, Y. Zhang, High efficient adsorption for thorium in aqueous solution using a novel tentacle-type chitosan-based aerogel: Adsorption behavior and mechanism. Int. J. Biol. Macromol. 222, 1747–1757 (2022).
48. C. Zhang, X. Li, Z. Jiang, Y. Zhang, T. Wen, M. Fang, X. Tan, A. Alsaedi, T. Hayat, X. Wang, Selective immobilization of highly valent radionuclides by carboxyl functionalized mesoporous silica microspheres: Batch, XPS, and EXAFS analyses. ACS Sustainable Chem. Eng. 6, 15644–15652 (2018).

Figures

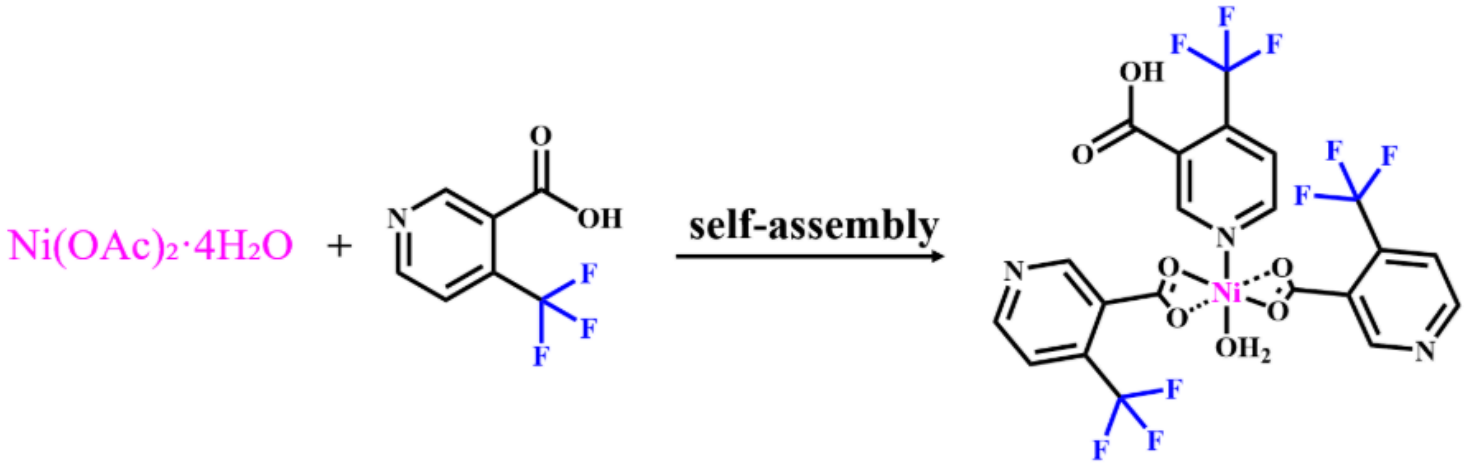


Figure 1

Synthesis route of Ni-tfc-CP.

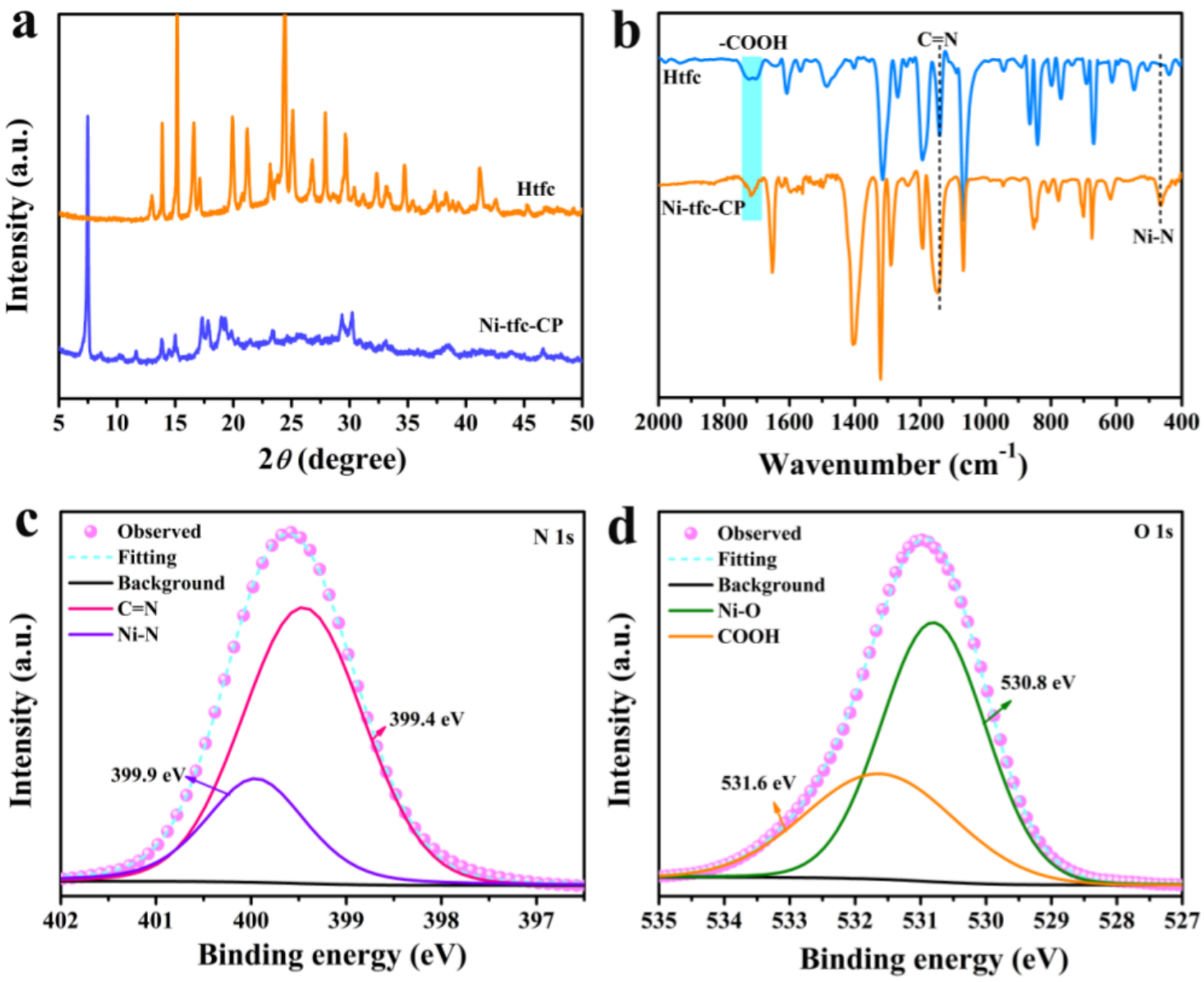


Figure 2

a XRD pattern of Htfc and Ni-tfc-CP, **b** FT-IR spectra of Htfc and Ni-tfc-CP, **c** N 1s XPS spectra of Ni-tfc-CP, **d**O 1s XPS spectra of Ni-tfc-CP.

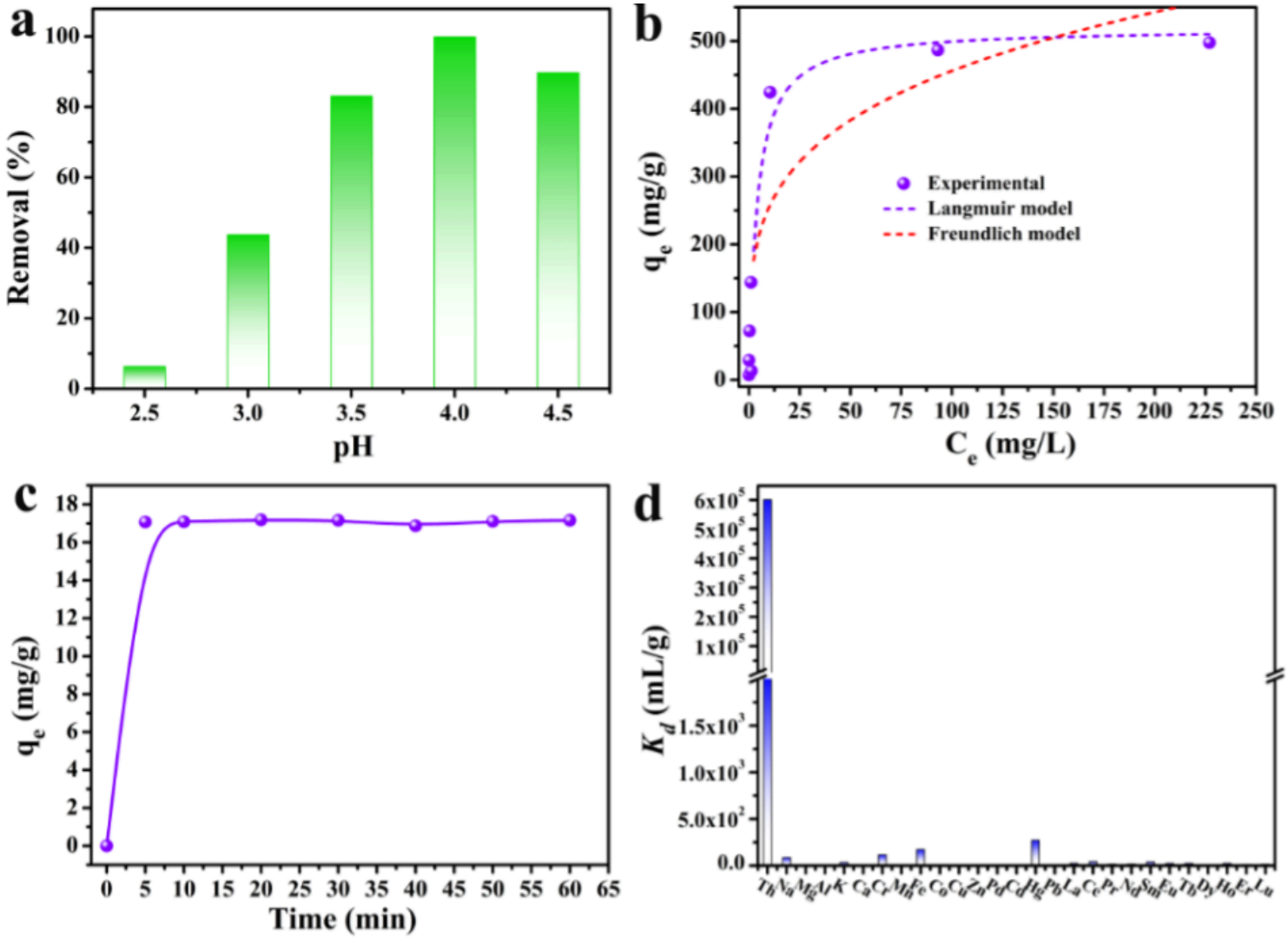


Figure 3

a Results of pH-dependent removal of Th(IV) at Ni-tfc-CP, **b** Adsorption isotherms of Ni-tfc-CP for Th(IV) fitted by the Langmuir and Freundlich models, **c** Adsorption kinetics of Th(IV) on Ni-tfc-CP, **d** Distribution coefficients (K_d) of Th(IV) and coexisting metal ions on Ni-tfc-CP.

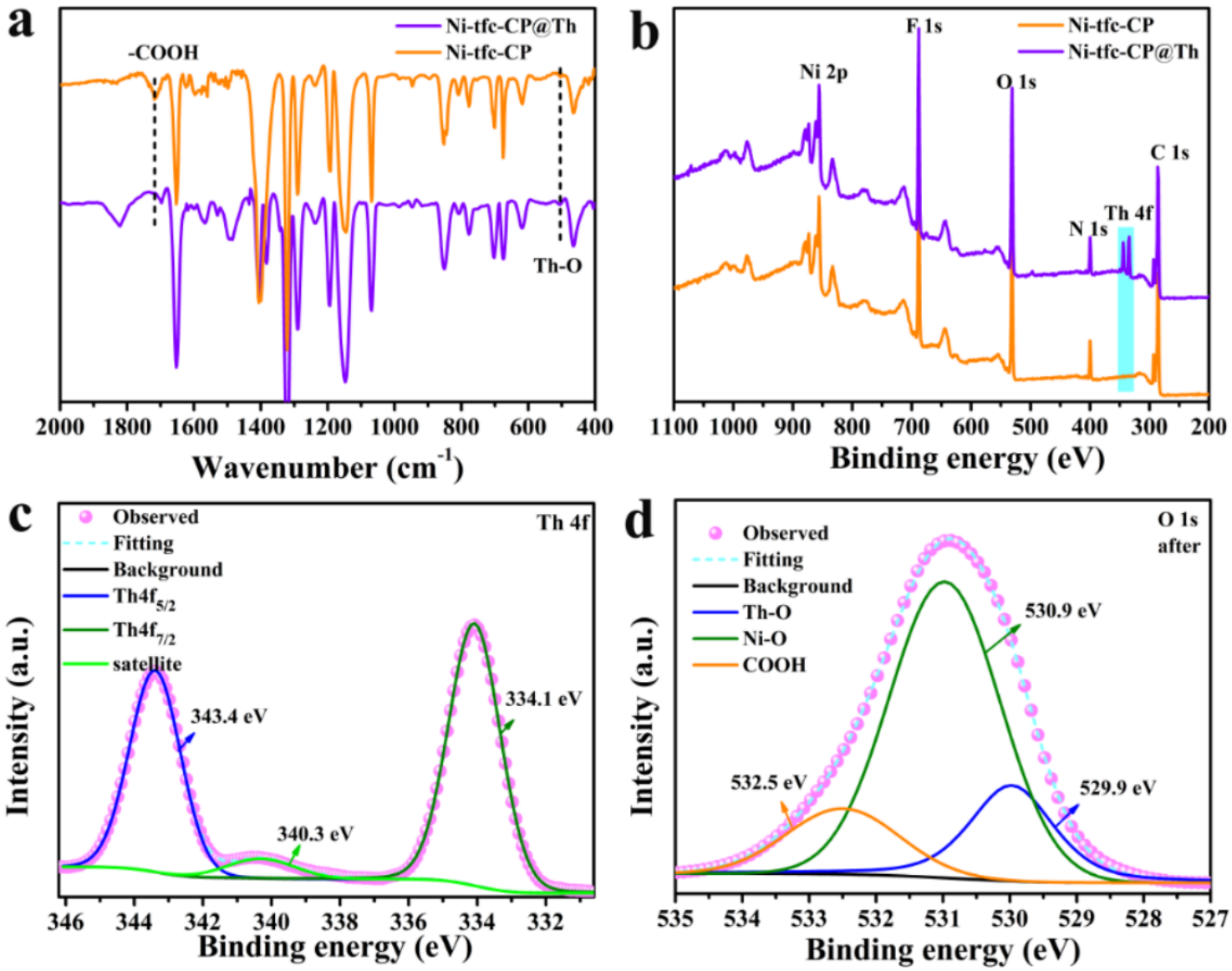


Figure 4

a FT-IR spectra and **b** XPS spectra of Ni-tfc-CP before and after Th(IV), **c** The deconvoluted peaks of Th 4f in Ni-tfc-CP after Th(IV)-adsorption, **d** XPS O1s spectra after Ni-tfc-CP adsorption of Th(IV).

Supplementary Files

This is a list of supplementary files associated with this preprint. Click to download.

- SupportingInformation.docx